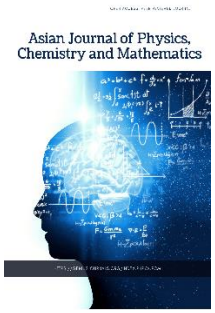

Estimation of structure, characterization and studying properties of novel CuNiSnSex nanocomposits

Muhamad L.Ali
Department of Physics, College of Science, University of Kirkok, Iraq
Dr mohanad44@uokirkuk.edu.iq

Mohanad Q.Karem
Department of Physics, College of Science, University of Kirkok, Iraq
Dr mohanad44@uokirkuk.edu.iq

ABSTRACT

CunisnSe nanocomposits were successfully synthesized in this study using the nanometric approach. It possesses a monoclinic structure and a hexagonal phase, according to XRD diffraction data. The tiny crystal size of CunisnSe causes the XRD line to expand. However, the comparison determined a significant number of grid ratios. The The agglomerated and circular rectangular configurations nanocomposit were confirmed by FESEM pictures. The optimal energy gap, according to optical characteristics, is 1.25 e v. whech aids the thermoelctric performence of material or sorbeants in solar call aplications.

Keywords: Optical Properties, Electric Properties, XRD

1INTRODUCTION

Thin-film photovoltaic cells a type of solar cell that uses a thin layer a low-cost alternative to traditional photovoltaic cells, and they've ben widely employed Light energy is converted into electrical energy. Nanostructures' quantium confineament effect has sparked interest in a variete of applicatiuns. Over the last few decades, semiconductor nanocomposits have already been widely explored. Semiconductor nanoparticles' intriguing optical properties have positioned them as inescapable In the future, there will be a variety of energy sources. Photocatalysis, photovoltaics, sensors, and photodetectors are all examples of photocatalysis, Renewable energy have developed as a significant component of electricity generation, and other semiconductor nanocomposits applications are currently being explored. Although photovoltaics contributes significantly to this sector, cost reduction is one among the most popular challenging parts of remaining competitive with fossil fuels The level of energy swings when demand exceeds the upper limit on a daily basis of growth and approeches a cretical leval. The amount of enargy useed to construct new systeams is greater than the amount of energy transported to that location by those systems The efficiency of PV panel conversion in land-based photovoltaic (PV) systems is dependent on the area covered by the panelsPV panels are strewn across a vast region[1] . Given the lifespan of a PV panel, which has been in existence for more than 20 years Becaose of it highs abcorption coeffecient and the charge carriers' long mean free path, ternary and quaternary based chalcogenides have sparked a lot of scienatific and

technulogical intarest in the creation of then film solar cells. Cnsse-based materials from the chalcogenide family are frequently employed as solar absorbers because their straight bands gap may be adjusted from 1.05 eV to 1.69 eV by adding sulfur and/or gallium The selenium-based thin-film solar cells are among the most efficient thin-film solar cellsll of thes chalcugenide-based materials have bandgaps of Eg = 1.71 eV solar cells with high absorption coefficients of 105 cm Despite this, due to the considerable roughness of the samples, optical examination of then-films solar call mateerials employing S (spectroscopic ellipsometry) has proven challenging. In a selenium or Se environment, high temperature selenization processes can be reduced. or even abolished by utilizing CNSSe nanocomposits with set composition and crystalline structures. Furthermore, by altering the composition of the nanoparticles, the compostion of the printed film may be easily regulated all sizes. Several approaches for the manufacture of CNSSe and related nanoparticles have been reported, including solvotherma In the family of multicomponent chalcogenide semiconductors, ternary CuNiSnSe2 (CNSSe), a promising PV absorber material for thin film solar cells, has received a lot of interest[(2)] .

II. MATERIAL AND METHODS

Preparation The hydrothermal process was used to create CNSSe porous structures. In a typical procedure, 0.2938 g of Nicl cloride is dissolved in 10 mL water and magnetically stirred for 11 minutes to obtain a clear solution. (2,4,6) wt% Thase soluttions were plased in a stainlless stael autocleve with Teflon lining. a 100 mL capaecity, whaich was half-filled with distilled wter. maintaned for 6 hour Thase solotions were placied in a Tefllon-linead stainles stel autoclave. liner. s at 180°C, then cooled to room temperature CuNiSnSex Thean fillms were cleaned three times with distilled water and ethanol to neutralize the solution, and the product's surounding water was eliminated by drying it in the air for onee hoaur at 60 degrrees Celsinus. To observe the effect of selenum, the technique was carried out under similar settings (Se After that, the crystael structaure, morphologe, and optiecal properties well be studied. CuNiSnSex was thes naeme of the product containing Se, while CNSSe was the name of the end product without Se.Characterization Details : Continuous scan mode is used to get the X-ray diffraction line profile data (2 = 10-80) with CuK∝ (= 1.5406 A) room-temperature radiation using an X'Peert PRo (PAN analytical) in the Bragg–Brentano difractometer par focusing the arangement (θ/2θ geometry) (25 C°)[(3)]. The electrons emitted from the A 40 kV voltege and a 30 mA filament current were used to drive the cathode filament towards the anode plate (Cu). The optics of the diffraction beam include Solar slit of 0.04 rad, a fixed divering slit (0.8719 slit size), a reciving slit with a diameter of 0.110 mm and a scintillator detector To decrease the instrumental contribution to line broadening in XRD , the sammples are scenned in a step-by-step manner. of 0.05 deg of 2θ and a constant counting time of 1.5sec at each level. Under vacuum, field emission scanning electron microscopy was used to analyze particle size and shaepe (FESEM). A system for energy disparsive X-ray spectroscope has been instalied. (EDAX). Heat evaporation is used to join aluminum electrodes using the Edward coating unit and an appropriate mask placed on the CuNiSnSe's surface. High conductivity silver was used to make conections between the aluminum and a few copper wires. By creating a stainless steel evacuated closed chamber with a controllable hot plate, rotating at nearly 90 degrees. (10-11 mbar). a molti-pin feed thriough at the chambber's base provides electrical conections to the heater, thermocuple, and senasor electrodis. On the heater, the semple was placid and the electrical resstance of the sensor we measurred with a multimter.

III. DISCUSSION AND RESULTS

Figur 1 shows the XRD patern in pure streuctural studies. CNSSe and $CNSSe_x$ thin films made up of a mix (2, 4 ,6) % wt Se The hydrothermal process was used to create the content. As can be sean in Figre 1, all diffriction peakss of CNSSe are well suited to a tenorite

system's monoclinic structure. The major peaks can be found for (A) at (2θ = 27.2184º, 34.9058º, 45.6948º, 53.7103º, 39.1926º, 42.2145º, 46.1799º, 45.5945º, 51.2987º, 56.5742º) attributed to the (001) , (001) , (002) , (011) , (0012) , (207) , (213) , (116) , (218) , (2014) planes for a tetrahadrite structure . Showing a hexegonal-phasse $CNSSe_3$ formattion, whaich is in agraement with JCDS cerd No: 96-901-3008, 96-901-4521,01-076-1865. The major peaks can be found for (B) at (2θ = 32.532O, 34.4785º, 46.4767º, 56.6866º, 56.8576º,56.8898º, 31.3182º, 33.5637º, 36.1696º, 38.6949º, 39.4017º, 44.75º) attributed to the (010) , (002) , (011) , (110) , (0012) , (116) , (114) , (1112) , (213)A tetrhadrite structur's planes A heagonal-phase CNSe formation is shown., which it in agreiment with JCDS cerd No: 96-900-9245, 96-9008571,01-075-2018. and the highest peks are observed for (C) at (2θ = 24.6656º, 29.955º, 33.5535º, 36.7065º, 45.0079º, 53.0714º, 54.1312º, 54.5437º, 54.985º, 55.732º) attributed to the (009) , (020) , (111) , (200) , (121) , (112) , (703) , (500) , (752) , (905JCDS card for tetrahadrite structure planes No: 0-035-1150, 03-065-4652 shows a hexagonal Furthermore, because of its hexagonal form, the three -phase CNSS development, which is consitent with JCDS card No: 0-035-1150, 03-065-4652. In addition, In's hexagonal structure, Thee three patierns shows a Tatraggonal structures. The pettern for puure semple shows law crysttaline, the seacond and therd patternt at (2,4, 6) % wt. SE shows an intcrease in thes x-ray diffrection peeks have increased in intensity, indicatting impruved crestalline and a bigger nember of peak. The Indium oxide peaks appear smaller at half maximum, indiceting that the nikal oxide crystalines sizee is increasing at thir retio. It's probable that the rise prices has something to do with it. The catalysis of the CuNiSnSex-1 addition, which promotes crystal growth, is responsible for the crystalline size at this ratio. The widening of the peaks in X-ray diffraction suggests that ther size is in the nanu ranges[4]. The Schrer methud can be usead to estimmate the grein size of the particcles. It is stil usead to figure out what the "apprent" domein is widthsd physicals broadeing crest profiles since it is a vary simply expresion.

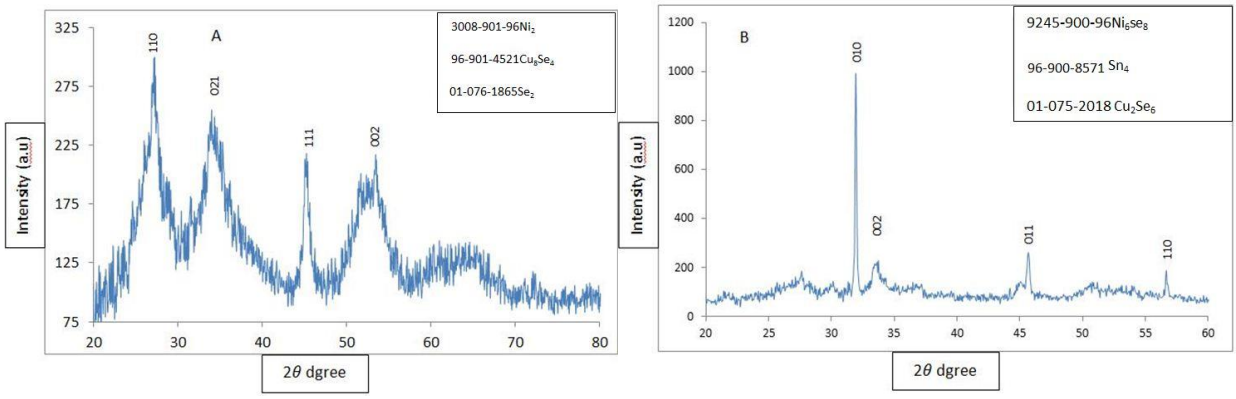

Using a hydrothermal method, glass surfaces were created and subsequently annealed at 180 degrees Celsius.

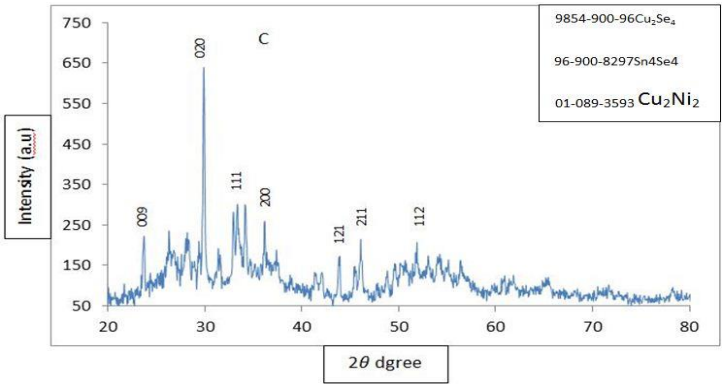

Fgure 1: XRD paterns of (A) CNSSe, (B) $CNSSe_3$, and (C) $CNSSe_2$ and (D) CNSSe nanocomposits was depossited on glass surfaces using techneque end then anealed an 180 degries Celius.

In this method, the crystallite size is calculated using the mean effect size of the coherently scattering region normal to the reflecting planes. The Scherer link between crystallite size and integral breadth is calculatd using the formula below.:

$$L = \frac{K\lambda}{\beta_L \, COS\theta} \quad , \beta_L = \frac{K\lambda}{L \, COS\theta} \qquad (1)$$

When L it the proper crystellite size it regard to the reflacting plene, Bd it the width of the integral of a specific peak, k is the furm factor (0.8), k it the wavelingth of CuK the reys, and K the wavelength on CuK the rays., and is thet eangle of diffrection Syze broedening it Eq. 1 shows that the order of a reflection is unaffected [5].The density of dislocations () can be calculated using the equation below. The dislocation line length per units avolume of the crystil is deefined as:

$$\delta = \frac{1}{L^2} \qquad (2)$$

Table 1 . CuNiSnSe@ (2 percent) Se structural characteristics, interplnar spcing, and crystaline size pure nanoparticle

Sample 2θ	FWHM [^{o}]	β(rad)	Hkl	d_{hkl}(A)	Scherrer method		standard card
					L_{sh}(nm)	δ(nm)$^{-2}$	
26.2184	0.96	0.016747	110	1.311	16.514	0.000136	4521-901-96 3008-901-96
34.9058	0.90	0.015700	021	2.16	24.986	0.000317	
45.6948	0.72	0.012560	111	3.287	28.525	0.000229	
53.7103	1.02	0.017793	002	2.16	27.371	0.000227	
39.0926	0.72	0.012560	106	1.459	49.002	0.001416	
41.2145	0.96	0.016747	207	1.401	35.508	0.000225	
45.1799	0.48	0.008373	213	1.258	12.223	0.003693	
45.594	0.84	0.014653	116	1.255	52.661	0.000255	
51.2987	1.14	0.019887	218	1.105	41.541	0.000279	
56.5742	1.20	0.020933	2014	0.999	33.892	0.000319	

Table 2 . CuNiSnSe@ (4 percent) Se structural charcteristics, interplanar spacing, and crystaline size of pure nanoparticle

Sample 2θ	FWHM [^{o}]	β(rad)	Hkl	d_{hkl}(A)	Scherrer method		standard card
					L_{sh}(nm)	δ(nm)$^{-2}$	
32.532	0.0984	0.001717	010	2.7717	41.8306	0.0002508	9008571-96 9245-900-96
34.4785	0.0984	0.001717	002	2.66	35.8529	0.0001529	
46.4767	0.3936	0.006866	011	2.78	33.1727	0.0028573	
58.6866	0.1476	0.002575	110	3.431	53.7704	0.0002458	
31.3182	0.1968	0.003433	0012	1.8030	39.9084	0.0004278	
33.5637	0.0984	0.001717		1.7250	59.3645	0.0002587	
36.1696	0.2460	0.004291	116	1.5846	41.5194	0.0010065	
38.6949	0.1800	0.003140	114	1.4416	32.7561	0.0003470	
39.4017	0.1800	0.003140	1112	1.4416	42.6627	0.0005494	
44.75	0.1200	0.002093	213	1.2861	42.8553	0.0055311	

Tabl 3 .Structural parmeters, interplnar spacing, crystaline size pure nanoparticle CuNiSnSe@ (6 %) Se

Sample 2θ	FWHM [^{o}]	β(rad)	Hkl	d_{hkl}(A)	Scherrer method		standard card
					L_{sh}(nm)	δ(nm)$^{-2}$	
24.6656	0.72	0.01256	009	2.842	31.1791	0.003229	9854-900-96 1303-901-96
29.9555	0.30	0.00523	020	2.320	22.5464	0.001739	
33.5535	1.20	0.02093	111	3.532	56.1561	0.000128	
36.7065	0.66	0.01151	200	2.515	41.9187	0.000582	
45.0079	1.08	0.01884	121	1.910	62.9505	0.000218	
53.0714	0.78	0.01360	112	1.792	34.0862	0.001664	
36.1312	0.96	0.01674	703	1.517	50.7775	0.000253	
39.5437	1.08	0.01884	500	1.440	61.0730	0.000398	
43.9885	0.60	0.01046	752	1.305	18.6052	0.005294	
51.7302	1.08	0.01884	905	1.124	47.9593	0.000417	

IV.FESEM Evaluation FSEM (field emission scanning microscop a versatile instrument for analyzng the morphology of materials. Micrographed nanoparticles of a tetahedrite CuNiSnSe structure created by hydrothermal method. (180C^o).

A

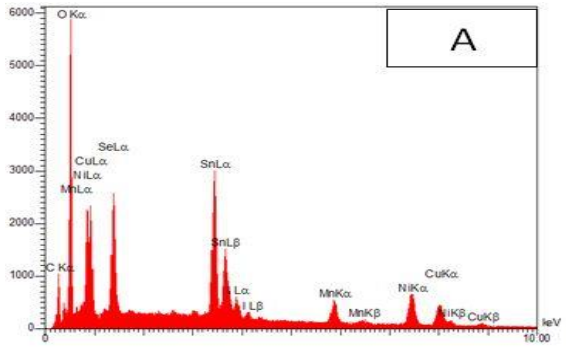

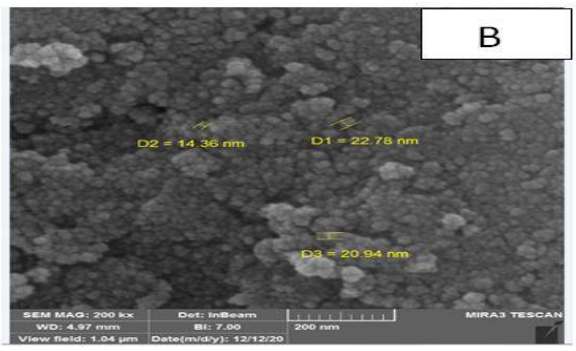

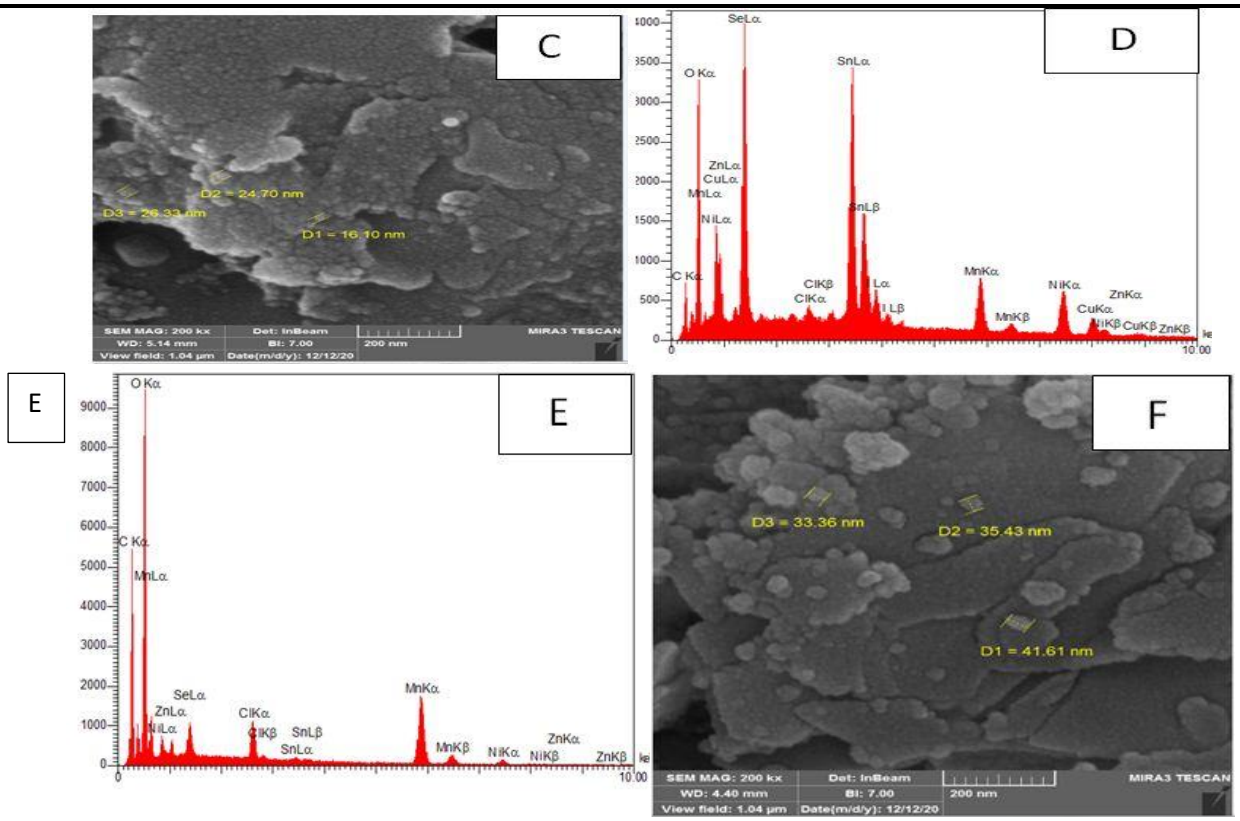

Figer 2 . FESEM images of CuNiSnSe nanoparticles generated by hydrothrmal technique and annealed at 180°C (a, c, and e) surface morphlogy (a , c, and e). (a, b, d, and f) CuNiSnSe nanoparticles Analyzed with EDX

It provides a homogeneous size distribution with agglomerates and a rectangle-like shape in sizes smaller than 29.84nm obsrved . It also verifies that the particles are on the nanoscale. EDS techniques were used to analyze the nanoparticles' precise microstructure. EDS analysis of the CuNiSnSe as seen in hexahedral nanoparticles Feg.2 (b ,d and f). two peeks coresponding in the coper (cu) peek observad. located at about 0.9, in 8.9 Kev corresponding to l∝ and K∝, Kβ transitionsand so forth. Whereas the nikle (Ni) peak arived at around 3.4 & 3.5 kev, reching the L and K transitions, the selenum (Se) peek appiared at about 3.31 & 3.51 Kev, reaching the L in K transitions. L transitions correspond to 1.4 Kev. They were inspecting the glass substrate as well as the height[6]. especially for (PEG), and (Na) peaks. The weight percentage ratio and atomic weight were calculated using an app that was coupled to the inspection device.

V. Optical Qualities

In terms of wavelengths, Uv-Vis absorbance speactra wean used to detarmine the film's optecal absorption. (300-1200) nm at room in the visible temperature portion of the electron 2enetic spectrum, and in the infrared region The optical absorbance value decreases as the wavelength rises, as seen in Figure 3. Cu Ni & Se Film optical absorption coefficient (α) photun enargy ($h\ v$)[7]. Thet preparid then film louked to heve a lyght valuy it > 10* cm-1. There indicetes thit streight truncattions are permittedThe bandgap energy can be calculated using the tuce formale. (Eg).:

$$B = \frac{(\propto h\nu)}{(h\nu - Eg)^r} \quad (3)$$

$$\alpha = B\frac{(h\nu - Eg)^r}{h\nu} \quad (4)$$

(hv) The photon energy is represented by, while the absorption coefficient is represented by. The energy in the bandgep is

(eg). (CuNiSnSe) has a permittid diract gap transiteons it the opticel bend (R=2), where (r) is e nomerical value value thit signifies the transition type's perriod, weth (r) denoting dyrect transetions end (r) denoting transitions that are not straight. Figre 3 depicts the variatiun of (hv) vs (hv) for thet (CuNiSnSe) then film..

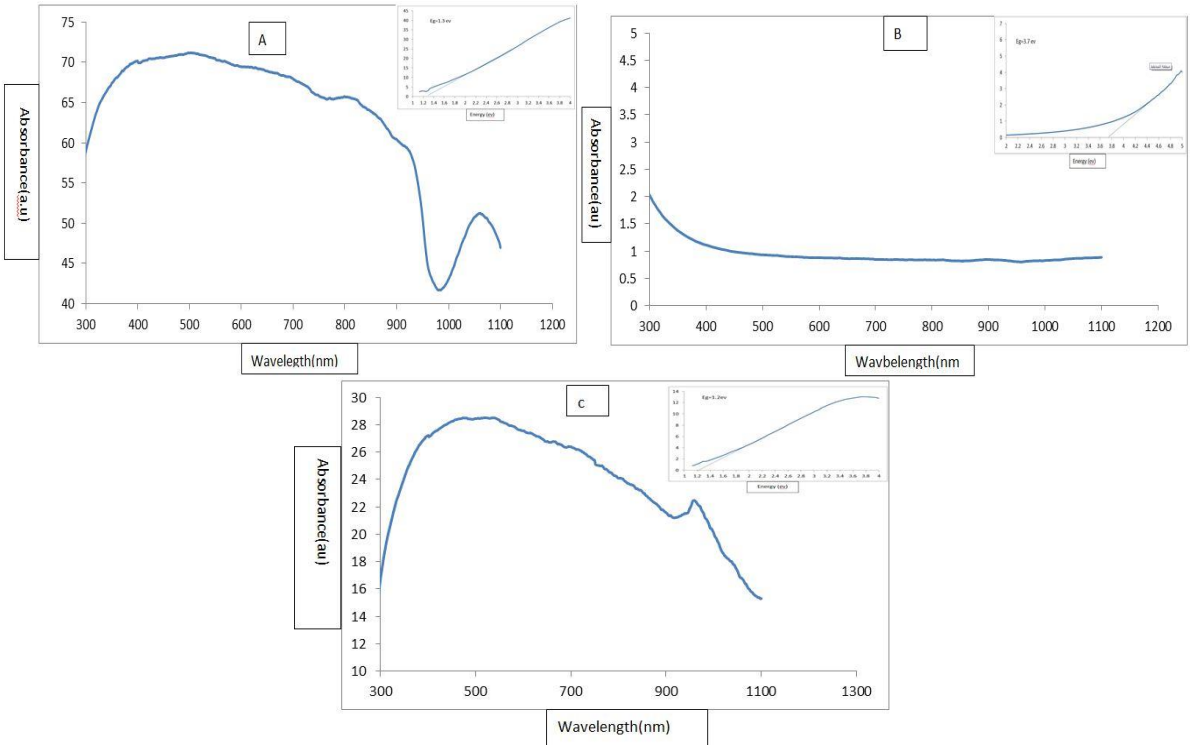

Figr 3 uV-ViS spectra were usid to detarmine the optecal charcteristics of the thrae CuNiSnSe nanoparticlas (a, b, and c) as wel as the enargy gip.

The bendgap enargy (eg) is bout a (1.3 ev); b (2.21ev) ; and c (1.8ev) the best and near is A for soler cill and photuvoltaic applicetions end thirmoalectric materials deveces.

V I. The Hall's Infloence

The Hell efect it defened as a phenomenon that occurs when two or more objects collide. production a perpendicular magnetic field that is perpendicular to the magnetic field applied. over an electrical wire, transverse to the current voltage differential (the Hall voltage). Author Edwin Hall is well-known. It was first the discovery of year 1869. Where a specymen is placed it the existence of a magnnet that is perpandicolar to that direction of curreant flew, an electricc fiald EY forms acruss thte spycimen it a both the magnetic field and the current in a perpendicular directionThis field is Hall field is what it's called. A perpendicular magnetic field is used to determine the Hall coefficient (RH). b to the electric fieeld, which results in currynt (I) (R_H) [8] .

$$R_H = 1/nq \quad \text{..... (5)}$$

The equation below relates the carriyr densite tu the Hill voltaege, The electron charge is q, and the carryer densety is

$$n = \frac{B}{qt} * \frac{I}{V_H}$$

..... (6)

Where: a measurement of the thickness of a film And the mobility of carriers e or h is determined by the type of carrier, such as electron or hole., $\mu_{e,h}$ is calculated by**:**

$$R_H = \frac{\mu_{e,h}}{\sigma_{e,h}}$$

..... (7)

Where

$$\sigma_{e,h} = nq\mu_{e,h}$$

..... (8)

The type of semicondctor under inquiry is determined by the sign of the Hall coefficient (RH)..

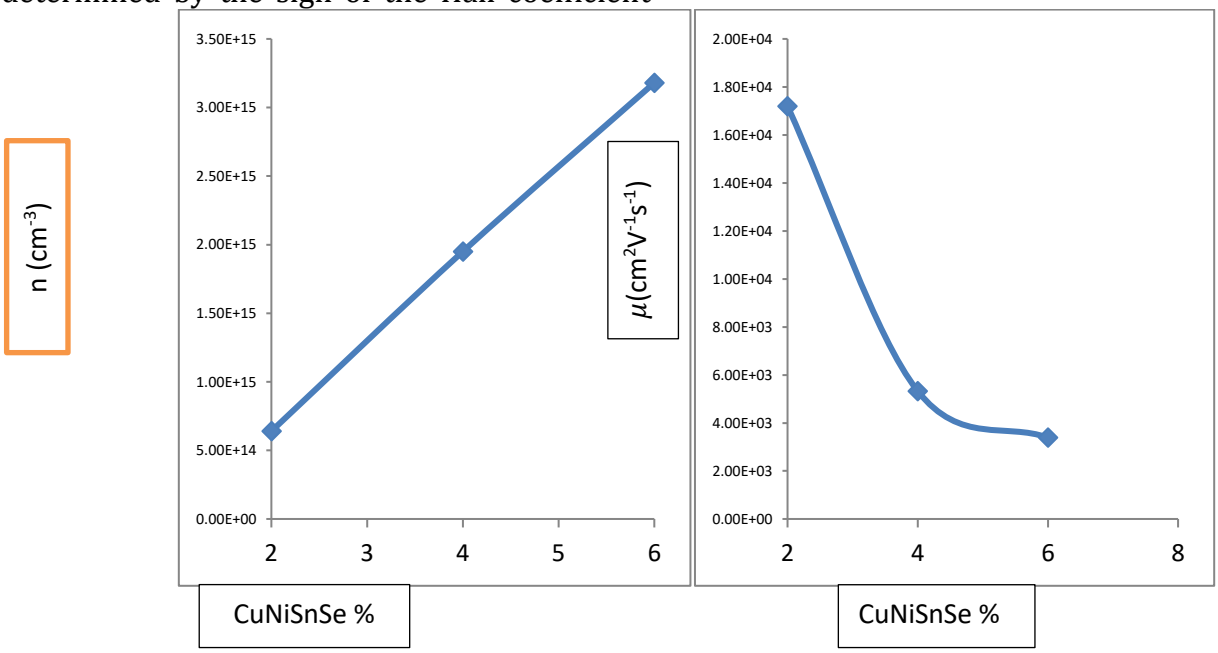

Figar(4) There greph shoews (A) Varietion of carryer conentration (n) with a dopent ratioa of Se@(2,4 and 6)%wt. CuNiSnSe$_x$ thain felms at tempereture 180˚C. (b) Varation of Mobilite with the depant ratios of Se@(2,4, and 6)%wt. CuNiSnSe$_X$ than films at temprature 180˚C.

All It Thase Thin Felms Exhibit A Posityve Hell Modolus, According To Hall Measurements (P-Type Cherge Carryrs). He Or She It Is Due To The Fallowing To Factors.

1- Abuve the condoction bends, the namber of electrons excited it greater than the number of holes. is stimulating below .

2- The lifetimes of fre elactrons boosted frum a negetive defects stete is longer thin the liffetime of fre holeas boosted fram a negative defact stite.

Table (4) The result of Hall experiment for CuNiSnSe thin films

CuNiSnSe$_x$ %	R_H (cm^{-3}C^{-1})	σ (o.cm)$^{-1}$	n (cm^{-3})	μ(cm^{2}V^{-1}s^{-1})
2	9.75E+03	1.77E+00	6.40E+14	1.72E+04
4	3.19E+03	1.67E+00	1.95E+15	5.33E+03
6	1.96E+03	1.73E+00	3.18E+15	3.38E+03

The structore of the then film was changed upon addition of Se, As a result, it could be inextricably connected to a growth in size of a very thin film grains, whereas in c1, the conductivity decreases with an increase in c. This behavior can be explained according to what is given in ref, that the thin film's structure was altered to lower grain volume while increasing the barrier potential of the inner grains, resulting in capture vectors. change in grain wrapbing then incryse dispearsion. The film gives p-tyape condoctevity op to c3, and one cuncludes thare these machine are lyttice dispertsion and grain boundary disparsion end the effectt of impuritys disparsion in the mobality of then fialms[10].

VII..Conclusion

In this study, CuNiSnSe A nanometria technique was used to successfully produce nanocompsit. It comes with a monoclinic structure and hexagonal phase, according to XRD diffraction data. The tiny crystal size of

CuNiSnSe causes the XRD line to expand. However, the comparison revealed a high number of retinal ancestry. The synthesis of Se from agglomerated rectangular nanoparticles and circular nanoparticles was confirmed by FESEM images. Based on optical properties, the energy gaps of A, B, and C were determined to be 1.3 ev, 2.21 Ev, nd 1.8 ev, respectively, whiach enhances there thermolactric performence of matarials or serbents in solar call applycations(12).

References

1. 1.A.R. Inigo, P.J. Skabara, Nanoparticles of Cu2ZnSnS4 as performance-enhancing additives for organic field-effect transistors, J. Mater. Chem. C 4 (2016) 5109d5115.
2. C. Coughlan, M. Ibanez, O. Dobrozhan, A. Singh, A. Cabot, K.M. Ryan, Compound copper chalcogenide nanocrystals, Chem. Rev. 117 (9) (2017) 5865e6109.
3. N. Singh, V. Murugadoss, S. Nemala, S. Mallick, S. Angaiah, Cu2ZnSnSe4 QDs sensitized electrospun porous TiO2 nanofibers as photoanode for highperformance QDSC, Sol. Energy 171 (2018) 571e579.
4. S. Yuan, S. Wang, L. Li, Y. Zhu, X. Zhang, J.m. Yan, Integrating 3D flower-Like hierarchical Cu2NiSnS4 with reduced graphene oxide as advanced anode materials for Na-Ion batteries, ACS Appl. Mater. Interfaces 8 (2016) 9178e9184.
5. M. Krishnaiah, S. Mallick, P. Bhargava, Alternative quaternary chalcopyrite sulfides (Cu2FeSnS4 and Cu2CoSnS4) as electrocatalyst materials for counter electrodes in dye-sensitized solar cells, J. Power Sources 305 (2016) 134e143.
6. M. Krishnaiah, S. Mallick, Effect of annealing atmosphere on quaternary chalcogenide-based counter electrodes in dye-sensitized solar cell performance: synthesis of Cu2FeSnS4 and Cu2CdSnS4 nanoparticles by thermal decomposition process, RSC Adv. 7 (2017), 18892-18892.
7. K. Mokurala, S. Mallick, P. Bhargava, S. Siol, T.R. Klein, M.F.A.M. van Hest, In-fluence of dipping cycles on physical, optical, and electrical properties of Cu2NiSnS4: direct solution dip coating for photovoltaic applications, J. Alloys Compd. 725 (2017) 510e518.
8. Ali, J. Jacob, A. Ashfaq, M. Tamseel, K. Mahmood, N. Amin, S. Hussain, W. Ahmad, U. Rehman, S. kram, D.S.A. Othmany, Modulation of structural, optical and thermoelectric properties of sol-gel grown CZTS thin films by controlling the concentration of zinc, Ceram. Int. 45 (2019) 12820e12824.
9. J. Sun, Y. Hu, K. Liao, C. Tang, Y. Lang, J. Xu, L. Zhao, W. Zhou, Q. Wang, K. He, The effect of the Zn/Sn ratio on the formation of single-phase kesterite Cu2ZnSnS4 solar cell material, Ceram. Int. 43 (2017) 8103e8108.
10. M.C. Johnson, C. Wrasman, X. Zhang, M. Manno, C. Leighton, E.S. Aydil, Selfregulation of Cu/Sn Ratio in the synthesis of Cu2ZnSnS4 films, Chem. Mater. 27 (2015) 2507e2514.
11. T. Tanaka, A. Yoshida, D. Saiki, K. Saito, Q. Guo, M. Nishio, T. Yamaguchi, In-fluence of composition ratio on properties of Cu2ZnSnS4 thin films fabricated by co-evaporation, Thin Solid Films 518 (2010) S29eS33.
12. Mohanad Q. Kareem, 2,Nadim K. Hassan" Evaluation of Williamson–Hall strain and Electrical properties in WO3@NaDCC/ITO nanoparticles thin films prepared by Hydrothermal method" September-October 2019 ‖ PP 16